applied sciences

MDPI

*Article*

# Mechanism of Removal of Hexavalent Chromium from Aqueous Solution by Fe-Modified Biochar and Its Application

**Run Pan, Jiangping Bu, Guoyu Ren, Zihao Zhang, Kexin Li and Aifang Ding ***

School of Environmental Science, Nanjing Xiaozhuang University, Nanjing 211171, China; runpan2-c@my.cityu.edu.hk (R.P.); 19050201@njxzc.edu.cn (J.B.); 18050110@njxzc.edu.cn (G.R.); 18050213@njxzc.edu.cn (Z.Z.); 18050222@njxzc.edu.cn (K.L.)
* Correspondence: dingaifang@njxzc.edu.cn

**Abstract:** This study discussed the mechanism of Fe-modified biochar (FeBC) derived from rice straw biochar (BC) as an adsorbent for removing Cr(VI) from aqueous solution and assessed its applicability in actual industrial wastewater. The Cr(VI) removal percentage increased with the FeBC dose, which achieved a removal of 99.5% at 8.0 g/L FeBC. Increasing the solution pH from 2 to 10 slightly reduced Cr(VI) adsorption by 6.6%. Coexisting ions such as $Ca^{2+}$, $Na^{+}$ and $Cl^{-}$ inhibited the removal of Cr(VI); the removal rate decreased to 60% at their concentration of 0.25 mol/L. The adsorption isotherm and kinetics were better described by the Langmuir isotherm and pseudo-second-order kinetic models, respectively. Through scanning electron microscopy with energy dispersive X-ray, the Brunauer–Emmett–Teller method, Fourier transform infrared, X-ray diffraction and X-ray photoelectron spectroscopy, the analysis revealed that FeBC with iron oxides loaded onto its surface had more active sites than BC; the surface functional groups changed; the removal of Cr(VI) by FeBC was mainly attributed to electrostatic adsorption; the redox reaction of Cr, and Fe loaded onto BC enhanced Cr(VI) reduction process. FeBC showed a good removal performance on actual industrial wastewater with the concentration of both total Cr and Cr(VI) meeting the integrated wastewater discharge standard of China.

**Keywords:** ferric nitrate; modified biochar; adsorption; hexavalent chromium; industrial wastewater



**Citation:** Pan, R.; Bu, J.; Ren, G.; Zhang, Z.; Li, K.; Ding, A. Mechanism of Removal of Hexavalent Chromium from Aqueous Solution by Fe-Modified Biochar and Its Application. *Appl. Sci.* **2022**, *12*, 1238. https://doi.org/10.3390/app12031238

Academic Editor: Juan García Rodríguez

Received: 25 November 2021
Accepted: 10 January 2022
Published: 25 January 2022



## 1. Introduction

Chromium (Cr) is a typical heavy metal pollutant in industrial wastewater, mainly from metallurgy, electroplating, leather tanning, mining, wood preservation and textile industries [1]. It predominantly exists in the trivalent chromium (Cr(III)) and hexavalent chromium (Cr(VI)) oxidation states in the environment. Cr(VI) poses a great threat to human health and the ecosystem due to its higher solubility, mobility and toxicity than those of Cr(III) [2]. At present, various techniques have been applied for the Cr(VI) removal, such as chemical precipitation, ion exchange, redox and adsorption. Among these techniques, adsorption is regarded as the most effective and simplest method to remove Cr(VI) from industrial wastewater [3,4].

It is critical for the adsorption method to obtain an adsorbent with low price, high adsorption capacity and easy accessibility. In the context of green chemical production, biochar has attracted the attention of researchers due to its economic and environmental sustainability. Biochar is a highly aromatic and carbonized solid matter formed from waste biomaterials by pyrolysis under the condition of oxygen deficiency [5]. Studies reveal that biochar has good adsorption capacity for heavy metal ions due to its well-developed pore structure, large specific surface area and negative charge. The efficiency of heavy metal removal by biochar is influenced by the properties and dosage of biochar, types and initial concentrations of heavy metals, and pH in aqueous solution [6,7].

Nascent biochar was relatively ineffective in removing oxyanions such as Cr, Se and As in aqueous solution. Thus, modifying the biochar to enhance its oxyanions adsorption

capacity has been explored [8,9]. Fe-modified biochar has been an inexpensive and highly effective method in enhancing Cr(VI) removal [10]. It has been shown that Fe-modified biochar has a good capability to remove Cr(VI) from acidic aqueous solutions [11,12]. Therefore, the pH of aqueous solutions was usually adjusted below 7 (e.g., PH = 2) in the treatment of wastewater containing Cr(VI), which caused acid pollution and increased treatment costs. In addition, some industrial wastewater often contain ions, e.g., $Ca^{2+}$, $Na^{+}$ and $Cl^{-}$, which may interfere with the adsorption and removal of Cr(VI) [13]. However, the efficiency of Cr(VI) adsorption and removal under such industrial wastewater conditions has been rarely studied.

Rice is widely grown in China; burning its straw in the open air will bring serious air pollution. Study on its recycling has been received wide attention. The aim of this study is to prepare Fe-modified biochar from rice straw biochar by impregnation method and to investigate the effect of different influencing parameters (i.e., modifier mass ratio, adsorbent dosage, pH and ionic strength) on the efficiency of Cr(VI) removal. Fe-modified biochar was characterized using scanning electron microscopy with energy dispersive X-ray (SEM-EDX), the Brunauer–Emmett–Teller method (BET), Fourier transform infrared (FTIR), X-ray diffraction (XRD) and X-ray photoelectron spectroscopy (XPS). Adsorption kinetics and isotherms were investigated in order to reveal the adsorption mechanism. This study will provide a theoretical basis and application for the Cr(VI) removal by Fe-modified biochar from industrial wastewater.

## 2. Materials and Methods

### 2.1. Materials and Reagents

Ferric nitrate nonahydrate ($Fe(NO_3)_3 \cdot 9H_2O$), $K_2Cr_2O_7$ and NaOH were purchased from Sinopharm Chemical Reagent Co., Ltd. All reagents used in the experiment were of analytical reagent grade and their solutions were prepared with deionized water (18.2 MΩ cm) using a Milli-Q water purification system (Millipore, MA, USA).

Biochar produced from rice straw under oxygen-limited conditions at 450 °C for 1 h was obtained from Sanju Biomass New Materials Co., Ltd., Nanjing, China. After washing with deionized water, drying, crushing and sieving through a 100-mesh nylon sieve, unmodified biochar for the experiment was obtained and labeled with BC.

### 2.2. Preparation of Fe-Modified Biochar

FeBC was prepared in 4 steps: (1) add BC to the $Fe(NO_3)_3$ solution at a solid-liquid ratio of 1:10 and set the mass ratio of $Fe(NO_3)_3$ and BC as 0.05, 0.1, 0.2, 0.3, 0.4, 0.5, 0.6 and 0.7, respectively); (2) react under continuously stirring in a water bath at 100 °C until drying; (3) wash reaction product with deionized water several times until no color appears in the washing solution after adding potassium thiocyanate, and (4) dry the reaction product at 105 °C after washing. The dried Fe-modified biochar was sealed in glass bottles and labeled with FeBC for further use.

### 2.3. Materials Characterization

The surface area and pore volume were investigated using an ASAP 2020 analyzer (Micromeritics, Norcross, GA, USA) and were calculated using the BET model at 77 K. BC and FeBC surface morphology was visualized using SEM (Regulus 8100, Hitachi, Japan) with EDX in order to evaluate their elemental composition. Functional groups on their surface were recorded by FT-IR spectroscopy (VERTEX 70, Bruker, Billerica, MA, USA) in the range from 400 to 4000 $cm^{-1}$ with a resolution of 4.0 $cm^{-1}$. Mineralogical characterization was investigated by powder X-ray diffraction (XRD) analysis (D8 Advance, Bruker, Billerica, MA, USA) with a copper target (Cu-K$\alpha$). The equipment was operated through step-scanning from 10° to 70° with a scan speed of $2° \cdot min^{-1}$ at 40 kV and 30 mA. The valence states of Cr and Fe species adsorbed onto the FeBC surface were analyzed by X-ray photoelectron spectroscopy (XPS) (AXIS Ultra DLD, Shimazu, Japan), and the XPS spectra were analyzed using XPS PEAK 4.1.

### 2.4. Batch Adsorption Experiments

Adsorption experiments were conducted with 25 mL Cr(VI) solution in 250 mL Erlenmeyer flasks. The effects of influencing factors on the adsorption performance were investigated separately, including modifier mass ratio (0.05–0.7), adsorbent dosage (1.0–10.0 $g \cdot L^{-1}$), solution pH (2.0–10.0), initial concentration (2–50 $mg \cdot L^{-1}$) and coexisting ionic strength. The initial pH was adjusted with HCl and NaOH solution. The effects of initial pH values on the Cr(VI) removal were assessed at a Cr(VI) concentration of 10 $mg \cdot L^{-1}$ and an adsorbent dosage of 8 $g \cdot L^{-1}$. The effects of initial Cr(VI) concentrations on the Cr(VI) removal were also performed at a pH of 6.0 and an adsorbent concentration of 8 $g \cdot L^{-1}$. Isotherm experiments were conducted at different initial Cr(VI) concentrations (5–70 $mg \cdot L^{-1}$) for 24 h at 298 and 380 K, respectively. Kinetic experiments were performed at different time intervals (i.e., 15, 30, 60, 90, 120, 150, 180, 240, 300, 360, 480 and 720 min) at 25 °C by adding 20.0 mg FeBC to 25 mL of Cr(VI) solution with initial Cr(VI) concentrations of 10 and 20 $mg \cdot L^{-1}$, respectively.

The flasks containing the adsorbent and the adsorbent mixture were placed in a digital thermostatic shaker and mixed at 150 $r \cdot min^{-1}$ for 2 h. Then, the mixtures were filtered with a 0.45 μm sieve. In addition, Cr(VI) concentration in the filtrate was determined by ultraviolet-visible (UV-vis) spectrophotometer (2800A, Unico Instrument Co., Ltd., Shanghai, China).

The Cr(VI) removal efficiency ($\eta$) and adsorption capacity ($q$) of BC and FeBC were calculated by

$$\eta = \frac{C_0 - C}{C_0} \times 100\% \quad (1)$$

$$q = \frac{C_0 - C}{W} \cdot \frac{V}{1000} \quad (2)$$

where $\eta$ is the Cr(VI) removal efficiency (%), $C_0$ and $C$ are the initial and residual Cr(VI) concentrations ($mg \cdot L^{-1}$), respectively, $q$ is the adsorption capacity ($mg \cdot g^{-1}$), $V$ is the solution volume (L) and $W$ is the adsorbent mass (g).

### 2.5. Adsorption Isotherm

Langmuir and Freundlich models were used to fit the isotherm studies. The two models are as follows [14]:

$$\text{Langmuir}: \ q_e = \frac{q_m K_L C_e}{1 + K_L C_e} \quad (3)$$

$$\text{Freundlich}: \ q_e = K_F C_e^{\frac{1}{n}} \quad (4)$$

where $C_e$ is the equilibrium concentration of solute ($mg \cdot L^{-1}$), $q_e$ is the amount of metal ions adsorbed at equilibrium ($mg \cdot g^{-1}$), $q_m$ is the maximum amount of metal ions per unit adsorbent to form a single layer ($mg \cdot g^{-1}$), $K_L$ is the isotherm constant related to the affinity of the binding sites, and $K_F$ and $n$ are the Freundlich constants related to the adsorption capacity and intensity, respectively.

### 2.6. Adsorption Kinetic

Pseudo-first order and pseudo-second order models were used to evaluate the experimental data and describe the adsorption kinetics. These two models are as follows [15,16]:

$$\text{Pseudo-first-order model}: \ \frac{dq_t}{dt} = K_1(q_e - q_t) \quad (5)$$

$$\text{Pseudo-second-order model}: \ \frac{dq_t}{dt} = K_2(q_e - q_t)^2 \quad (6)$$

where $q_e$ ($mg \cdot g^{-1}$) and $q_t$ ($mg \cdot g^{-1}$) are the amount of adsorbed solute at equilibrium and at time $t$ (min), respectively, and $K_2$ ($g^{-1} \cdot mg^{-1} \cdot min^{-1}$) and $K_1$ ($min^{-1}$) are constants of the pseudo-second-order and pseudo-first-order kinetic models.

### 2.7. Statistical Analysis

Each treatment was performed in triplicate; reagent blanks were also used to ensure the accuracy and precision of the analysis result. The mean and standard deviation (SD) values were calculated using the Microsoft Excel 2013.

## 3. Results and Discussion

### 3.1. Characterization of BC and FeBC

The surface area, pore volume and average pore size of BC and FeBC are listed in Table 1. As shown in Table 1, the BET surface area of FeBC (44.69 $m^2 \cdot g^{-1}$) was higher than that of BC (26.75 $m^2 \cdot g^{-1}$). The pore volume and average pore size of FeBC (i.e., 0.0351 $cm^3 \cdot g^{-1}$ and 5.50 nm) were also higher than those of BC (i.e., 0.0072 $cm^3 \cdot g^{-1}$ and 5.11 nm). This indicated that the Fe modification process allowed BC to provide a more developed pore structure and more active adsorption sites, thus reducing the mass transfer resistance in the adsorption process and facilitating the adsorption [17].

**Table 1.** Pore characteristics of BC and FeBC.

| Sample | Specific Surface Area /$m^2 \cdot g^{-1}$ | Pore Volume /$cm^3 \cdot g^{-1}$ | Average Pore Diameter /nm |
|---|---|---|---|
| BC | 26.75 | 0.0072 | 5.11 |
| FeBC | 44.69 | 0.0351 | 5.50 |

The surface morphologies of BC and FeBC through SEM images are shown in Figure 1. It can be found that, compared with BC, FeBC had a rougher surface and slightly damaged pore structure. Many fine flocculent solid particles with different sizes were observed on the surface and in the pores, which were dispersed, disorderly and partially overlapping (Figure 1b). The EDS spectra of BC and FeBC are shown in Figure 2. The absorption peak of Fe was found in the spectrum in FeBC (Figure 2b); it can be concluded that these particles may be iron oxides, indicating that Fe was successfully loaded onto BC.

XRD patterns of BC and FeBC samples are shown in Figure 3. The wide peak of BC and FeBC at $2\theta$ of 26.8512° were the characteristic peak of C with the highest intensity. No significant peaks were detected in the pattern of FeBC except for some relatively narrow peaks, suggesting that the crystalline Fe content was low and the amorphous structure was mainly loaded on the FeBC [18].

FT-IR was used to investigate the functional groups in BC and FeBC, as shown in Figure 4. The peaks detected in BC at about 3434, 2921, 1619, 1384, 1097 and 797 $cm^{-1}$ were attributed to the stretching vibration of the -OH, C-H, C=O in aromatic rings, -COO-, C-O-C and C-H groups, respectively. The Fe modification resulted in a shift of FT-IR absorption peaks and a decrease of the peak intensity, indicating that surface complexes of some groups (e.g., -OH and -COO-) formed with Fe (III) led to changes in the chemical environment around the groups. In addition, the decrease of the peak intensity was mainly attributed to the physical coverage of functional groups on the BC surface by iron oxides [19]. Nevertheless, the surface of FeBC still had abundant hydroxyl and carboxyl groups, which promoted the adsorption of heavy metals [20]. Furthermore, the abundant aromatic carbon provided electrons and enhanced the potential redox activity [21].

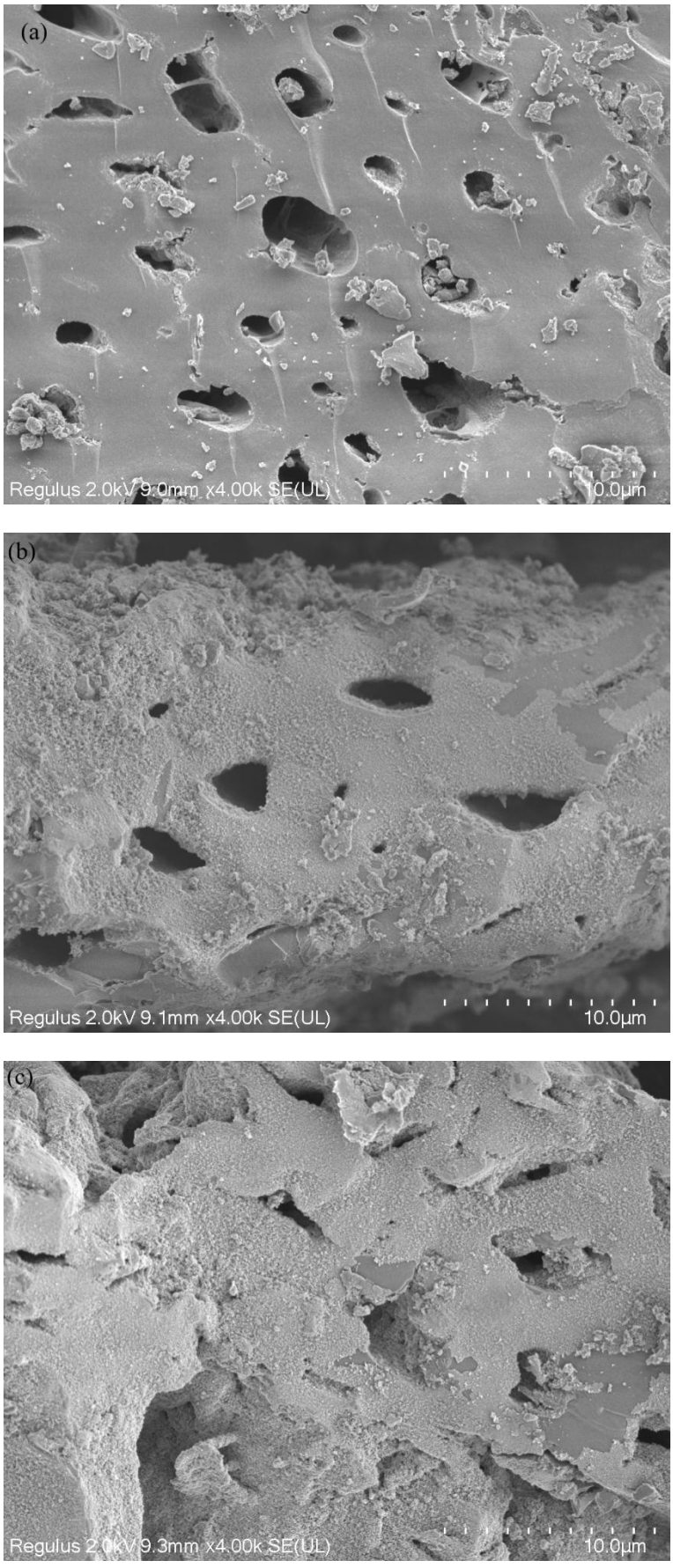


**Figure 1.** SEM images of (**a**) BC, (**b**) FeBC and (**c**) Cr-FeBC.

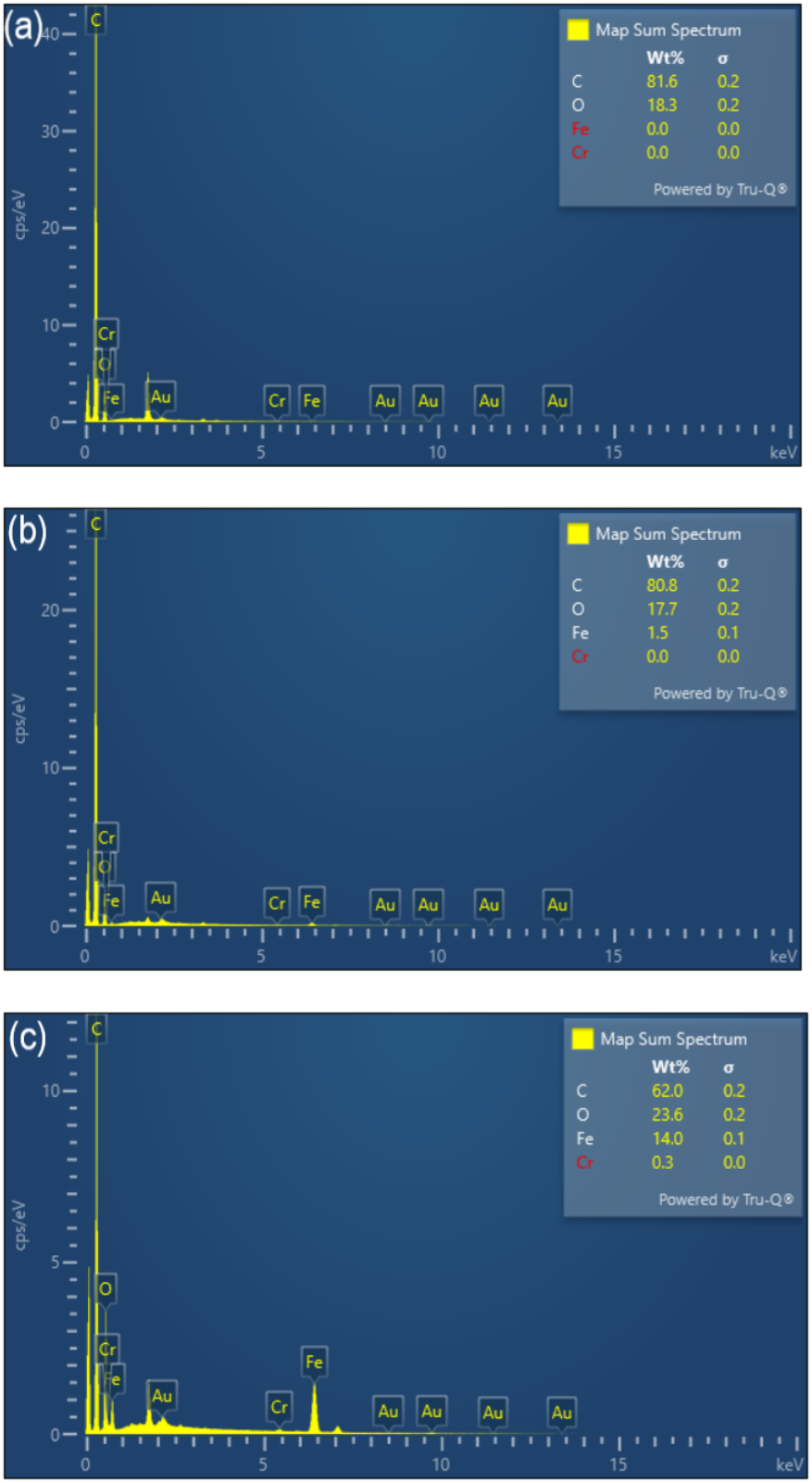


**Figure 2.** EDX spectra of (**a**) BC, (**b**) FeBC and (**c**) Cr-FeBC.

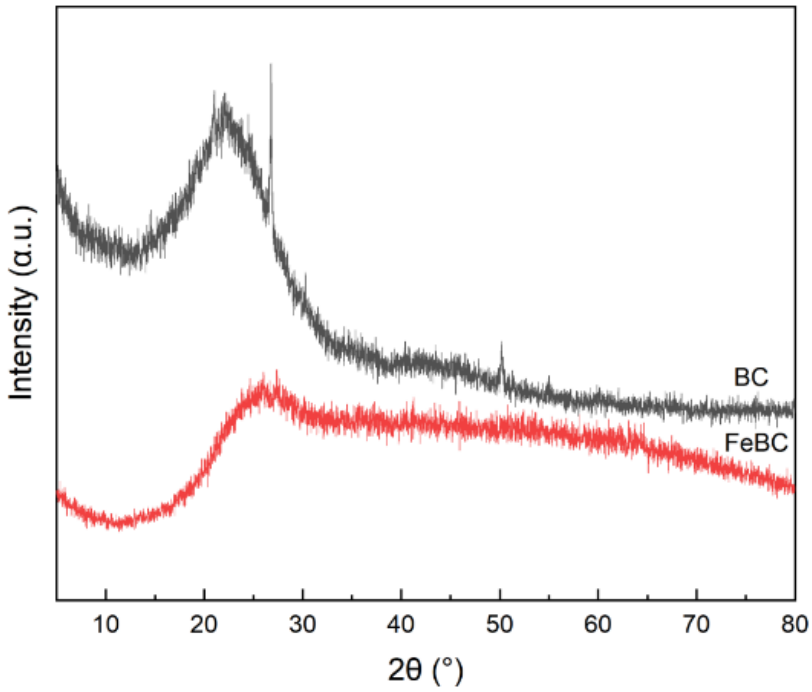


**Figure 3.** XRD patterns of BC and FeBC.

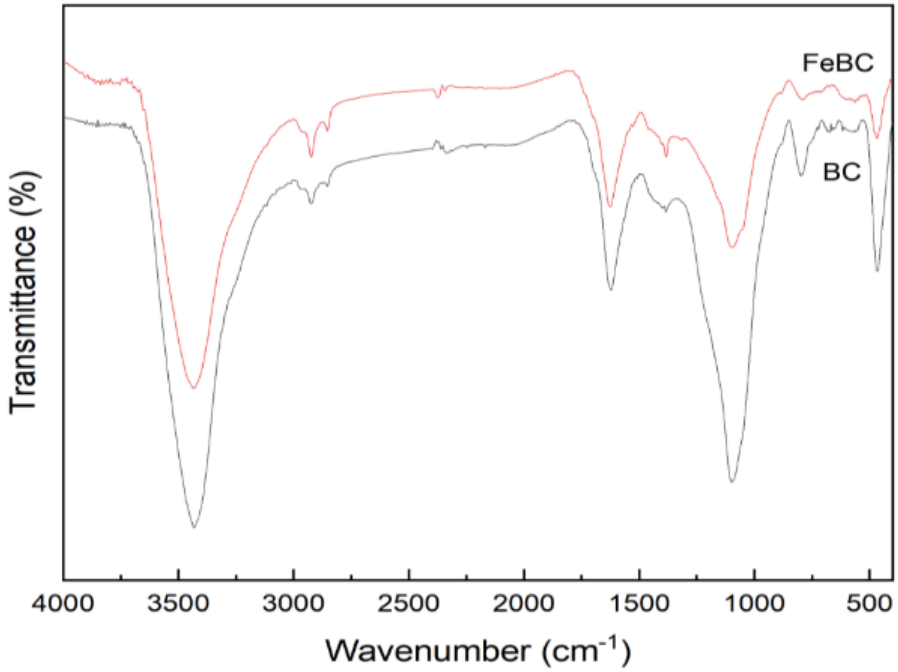


**Figure 4.** FT-IR spectra of BC and FeBC.

### *3.2. Effect of Modifier Mass Ratio and Dosage of FeBC on Cr(VI) Removal*

The removal efficiency of Cr(VI) by BC was only 4.57%, while the Cr(VI) removal capacity significantly increased due to the $Fe(NO_3)_3$ modification. The effects of modifier mass ratio on the Cr(VI) removal efficiency are shown in Figure 5a. FeBC, with a mass ratio ($Fe(NO_3)_3$/BC) of 0.4:1, showed the best adsorption effects with a removal efficiency of 99.5%. This implied that the modification of $Fe(NO_3)_3$ promoted the microstructure of BC and increased its adsorption sites. However, when the modifier mass ratio exceeded 0.4:1, the removal efficiency of Cr(VI) did not increase. This may be due to the fact that excess

metal ions blocked the formed micropore, indicating that the modifier mass ratio had the best modification effect within a certain range.

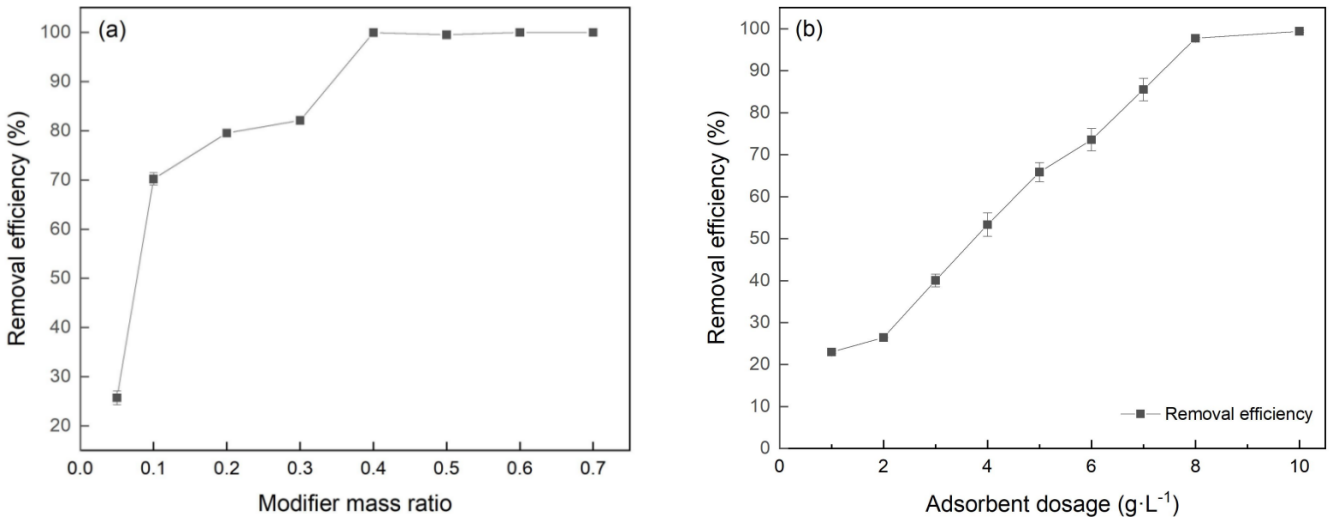


**Figure 5.** Effect of (**a**) modifier mass ratio and (**b**) dosage of FeBC on Cr(VI) removal.

A key factor affecting the Cr(VI), removal by FeBC was the dosage. As shown in Figure 5b, the removal efficiency increased from 23.9% to 99.9% with the FeBC dosage increasing from 1 to 10 g·L$^{-1}$. The increase of FeBC dosage provided more active sites, accelerating the removal rate and improving the removal efficiency [22].

### *3.3. Effect of pH and Initial Concentration on Cr(VI) Removal by FeBC*

The Cr(VI) removal efficiency of adsorbents with the initial pH ranging from 2.0 to 10.0 is presented in Figure 6a. The removal efficiency of Cr(VI) remained above 99.0% across the whole pH range from 2 to 5 and then slowly decreased with the pH increasing. The efficiency remained as high as 92.5%, even when the pH reached 10. The pH value affected the charge property of the adsorbent surface and the existing form of chromium in the solution [23]. In the acidic environment, the surface functional groups of adsorbents formed positively charged functional groups (i.e., -$OH^{2+}$ and -$COOH^{2+}$) because of hydroxyl protonation, which facilitated the adsorption of $HCrO_4^-$ and $Cr_2O_7^{2-}$ in the solution by electrostatic attraction [24,25]. Electrostatic attraction became weaker at higher solution pH due to the reduction of hydroxyl protonation on the adsorbent surface and the competition of $OH^-$ in the aqueous solution, resulting in the decrease of the Cr(VI) removal efficiency. In this study, the removal efficiency of Cr(VI) remained above 90%, with the solution pH ranging from 6.0 to 10.0, indicating that there existed other effects on the Cr(VI) removal efficiency. The reason may be that the Cr(VI) oxyanions can be reduced and Cr(III) precipitated as $Fe_nCr_{(1-n)}(OOH)$ and $Cr(OH)_3$ due to the oxidation/reduction reaction between Cr(VI) and FeBC [26,27].

The effect of initial concentration on the Cr(VI) removal by FeBC is shown in Figure 6b. The removal efficiency was kept at 99.0% with a concentration of Cr(VI) ranging from 2 to 10 mg/L, and decreased with the initial concentration of Cr(VI) increasing from 10 to 50 mg/L. Apparently, an adsorbent with a certain mass had a limited number of active sites and these sites progressively approached saturation as the Cr(VI) concentration increased. Thus, the saturated adsorbent cannot adsorb more Cr(VI) ions, which resulted in a decrease in removal efficiency in high concentration of Cr(VI) [28].

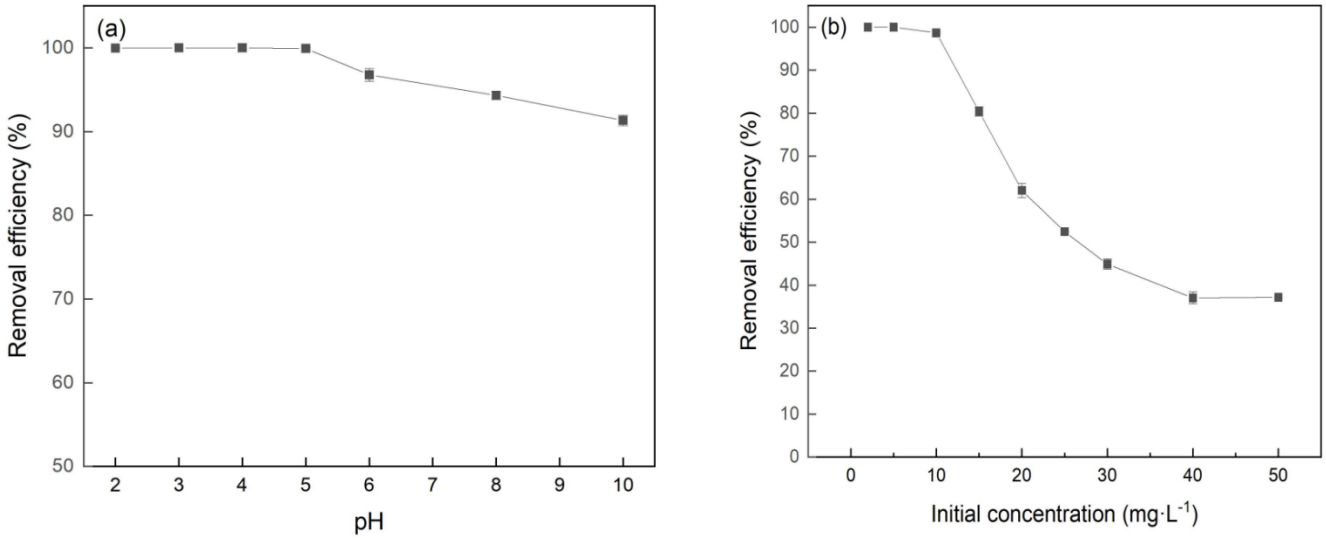


**Figure 6.** Effect of (**a**) pH and (**b**) initial concentration of Cr(VI) on the Cr(VI) removal by FeBC.

### *3.4. Effect of Coexisting Ions in Solution*

Due to the impact of production and other wastewater treatment processes, some industrial wastewater may contain lots of ions, e.g., $Ca^{2+}$, $Na^{+}$ and $Cl^{-}$ [29]. Therefore, ionic strength is also an important factor affecting the removal of Cr(VI). As shown in Figure 7, with an increase in the concentration of $Ca^{2+}$, $Na^{+}$ and $Cl^{-}$, the removal efficiency decreased from 90% to 60%. However, when the concentration was higher than 0.25 mol·$L^{-1}$, the efficiency decreased slowly. In terms of $Cl^{-}$, these may be associated with the fact that the competitive adsorption of $Cl^{-}$ or ions produced by its hydrolysis on the active sites of FeBC interfered with the adsorption of Cr(VI) on FeBC. In terms of $Ca^{2+}$ and $Na^{+}$, the main reason may be the electrostatic interaction weakened between the surface charge of FeBC and Cr(VI) ions in the presence of cations [30].

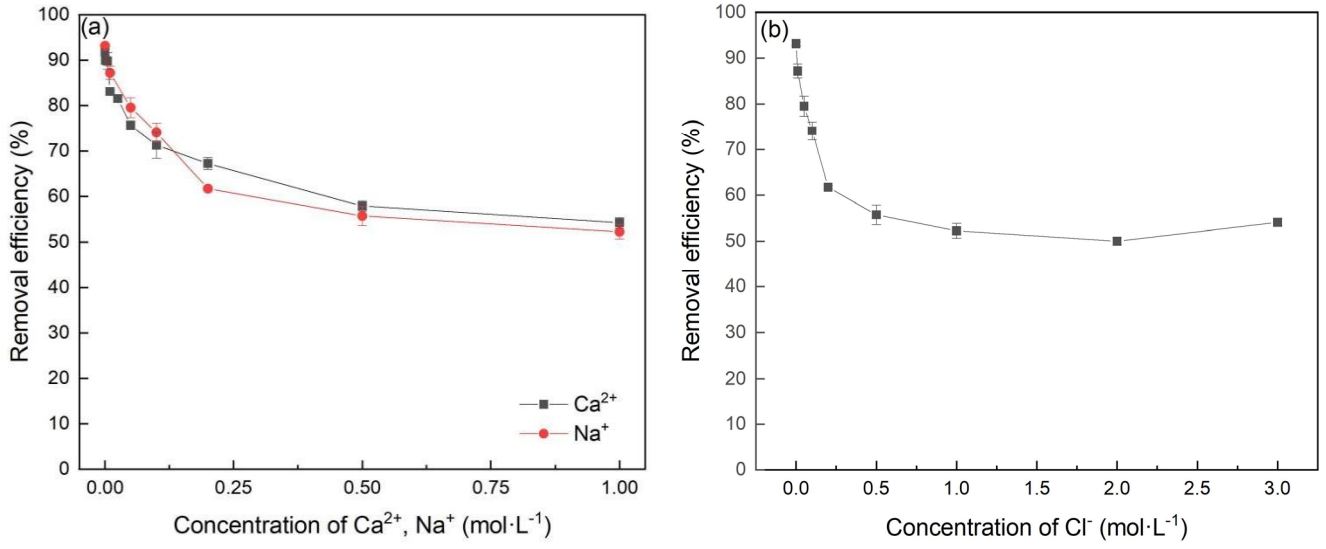


**Figure 7.** Effect of $Ca^{2+}$, $Na^{+}$ (**a**) and $Cl^{-}$ (**b**) in solution on the Cr(VI) removal by FeBC.

### *3.5. Adsorption Isotherms*

Table 2 and Figure 8 show that the two models fitted the experimental removal data well, and that the Langmuir model fit better with a higher value of $R^2$ (>0.99). The Langmuir model assumes that the adsorption of metal ions occurs through monolayer adsorption on a homogeneous surface without interaction between the adsorbed ions. However,

the Freundlich model is based on the adsorption on the heterogeneous surface [14,31]. It indicated that monolayer adsorption and heterogeneous surface conditions may coexist under the experimental conditions, but that monolayer adsorption was more dominant [32]. Besides, KL increased with increasing temperature, indicating that the adsorption of Cr(VI) onto FeBC was endothermic. Therefore, the higher temperature was beneficial to the adsorption process of Cr(VI) onto FeBC.

**Table 2.** Langmuir and Freundlich model parameters for the Cr(VI) adsorption onto FeBC.

| Temperature/K | Langmuir Model | | | Freundlich Model | | |
|---|---|---|---|---|---|---|
| | $q_m$/mg·g$^{-1}$ | $K_L$/L·mg$^{-1}$ | $R^2$ | $K_F$ | $n$ | $R^2$ |
| 298 | 2.7840 | 0.6001 | 0.9950 | 1.4606 | 5.8720 | 0.9310 |
| 308 | 3.0921 | 0.8398 | 0.9972 | 1.8098 | 6.8917 | 0.9304 |

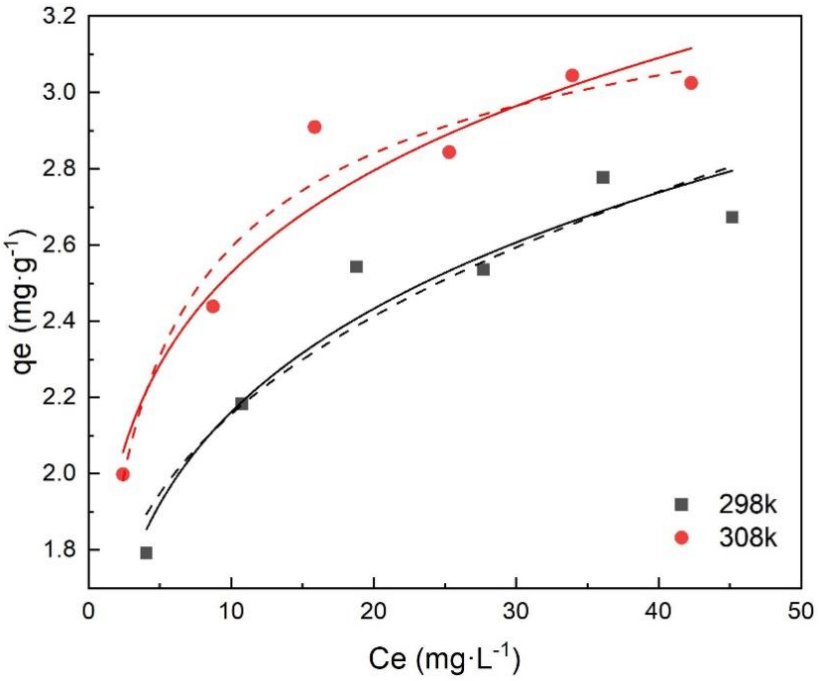


**Figure 8.** Langmuir isotherm (dash line) and Freundlich isotherm (solid line) for the adsorption of Cr(VI) onto FeBC.

### *3.6. Adsorption Kinetics*

The adsorption kinetic study was essential to determine the adsorption efficiency for practical applications [33]. As shown in Table 3 and Figure 9, the kinetic data were better fit by the pseudo-second-order model with a higher value of $R^2$ (>0.99). Besides, The calculated $q_e$ values (i.e., 1.216 and 1.787 mg·g$^{-1}$) by Equations (5) and (6) were close to the experimental values (i.e., 1.221 and 1.792 mg·g$^{-1}$), respectively, indicating the chemisorption involved covalent interaction due to the sharing and exchange of electrons between Cr(VI) ions; the chemical sorption process was the rate-limiting step of the adsorption of Cr(VI) onto FeBC [34].

**Table 3.** Pseudo-first-order model and pseudo-second-order model parameters for Cr(VI) adsorption by FeBC.

| Initial Cr(VI) Concentration/mg·L$^{-1}$ | Pseudo-First-Order Model | | | Pseudo-Second-Order Model | | |
|---|---|---|---|---|---|---|
| | $q_e$/mg·g$^{-1}$ | $K_1$/min$^{-1}$ | $R^2$ | $q_e$/mg·g$^{-1}$ | $K_2$/g$^{-1}$·mg$^{-1}$ min$^{-1}$ | $R^2$ |
| 10 | 0.2066 | 0.0085 | 0.9219 | 1.2211 | 0.1403 | 0.9998 |
| 20 | 0.5278 | 0.0046 | 0.9329 | 1.7918 | 0.0320 | 0.9982 |

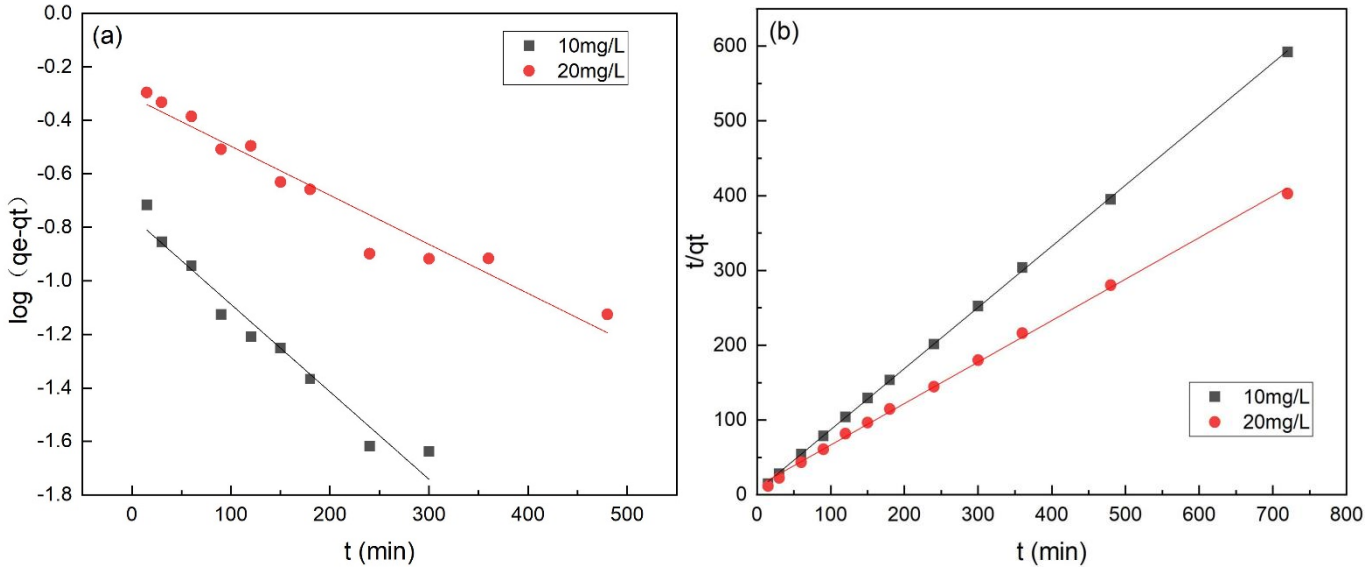


**Figure 9.** Pseudo-first-order model (**a**) and pseudo-second-order model (**b**) for the adsorption of Cr(VI) onto FeBC.

### *3.7. Proposed Adsorption Mechanism of Cr(VI) Removal*

The FT-IR spectra of FeBC before and after Cr(VI) adsorption are shown in Figure 10. After adsorption, the intensity of the peak at 1095 $cm^{-1}$ (C-O-C) increased. The peak at 1624 $cm^{-1}$ (C=O) shifted to 1619 $cm^{-1}$, with an increase in peak height, indicating the complexation of the carboxylic group with Cr. It was also observed that the peak at 1383 $cm^{-1}$ (-COOC-) was no longer significant; the intensity of the peak at 785 $cm^{-1}$ (C-H) increased, indicating that C-H bonds changed after adsorption. In addition, new peaks appeared at 672, 663 and 560 $cm^{-1}$, indicating the formation of Fe-O-Cr complexes between the Fe-O characteristic peak and Cr. These results indicated that C-O-C, C=O, -COOC- and C-H groups were involved in the adsorption, and C-O-C and C=O were the main groups on FeBC for the Cr(VI) removal from aqueous solutions [35]. After adsorption, the surface of FeBC became rough due to the coating of adsorbed Cr(VI) ions (Figure 1b,c). The EDX results (Figure 2) show that after the Cr(VI) removal process, the carbon losses of FeBC was 18.8%, while the content of Fe and O increased by 12.5% and 5.9%, respectively. A new peak characteristic of Cr (0.3%) was observed, indicating the successful combination of Cr and FeBC and the formation of more iron oxides during adsorption [36]. Therefore, surface adsorption or ion exchange may be responsible for the Cr(VI) removal process. XPS was used to examine surface structural information and elemental composition of FeBC before and after the Cr(VI) removal process (Figure 11). A new typical peak at the binding energy of 578.0 eV corresponding to Cr(VI) ions appeared in the total survey spectra, indicating the occurrence of Cr adsorption/precipitation onto FeBC. In addition, three peaks at 576.8, 578.0 and 579.2 eV in the high-resolution spectra of Cr2p were assigned to Cr(III)-O, Cr (III)-OH and Cr(VI)-O of $Cr_2O_3$, $Cr(OH)_3$ and $Cr_2O_7^{2-}$, accounting for 44.52, 29.22 and 26.26%, respectively [35]. The relatively high Cr(III) content (73.74%) indicated that Cr(VI) contributed significantly to the reduction rather than direct Cr(VI) adsorption [37]. The Fe spectra was also analyzed to further clarify the Cr(VI) removal process (Figure 11); it illustrated the peaks at 710.6 and 713.9 eV, the representative contents of Fe(II) (61.0%) and Fe(III) (39.0%) [38], and the nascent Fe(II) produced from the reduction of Fe(III) by BC. Fe(III) loaded on BC surface was reduced to Fe(II) in water, which directly reduced Cr(VI) to Cr(III), and then Cr(III) settled onto the FeBC surface. The resulting Fe(III) could be re-adsorbed onto BC and participate in the adsorption. Therefore, the reduction process could be the main mechanism of the Cr(VI) removal by FeBC and Fe played a strengthening role in the reduction process.

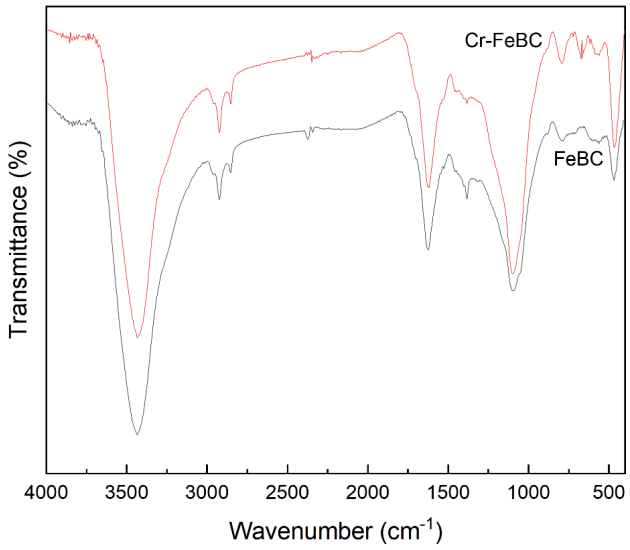


**Figure 10.** FT-IR spectra of FeBC before and after Cr(VI) adsorption.

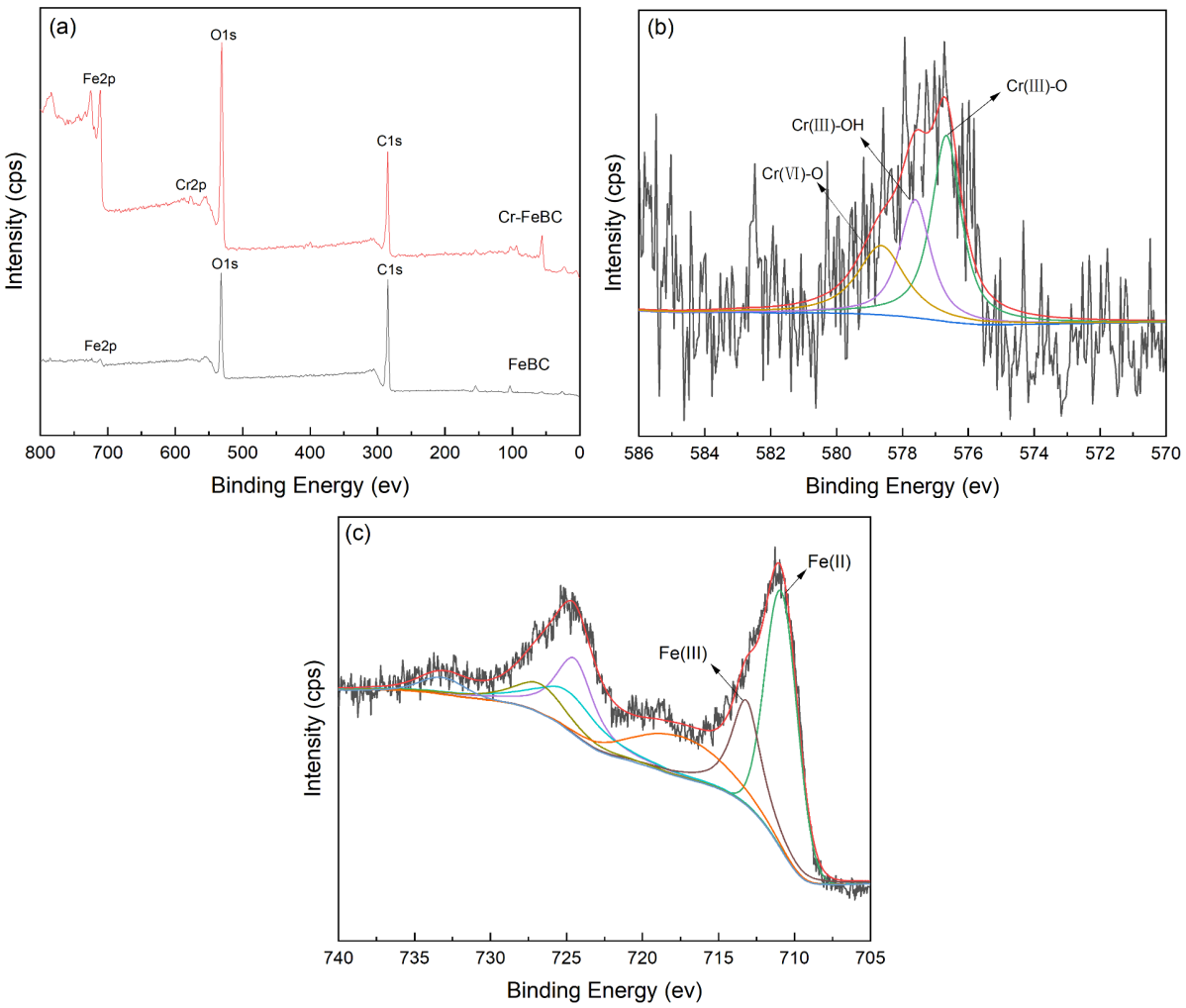


**Figure 11.** XPS spectra of FeBC. (**a**) The total survey spectra before and after Cr(VI) adsorption, and high resolution of (**b**) Cr2p and (**c**) Fe2p after Cr(VI) adsorption.

### 3.8. Removal Capability of FeBC in Actual Industrial Wastewater

In order to study the Cr(VI) removal performance of FeBC in actual wastewater, FeBC was used to adsorb electroplating wastewater at a dosage of 10 $g \cdot L^{-1}$; the results are shown in Table 4. Before treatment, the total Cr and Cr(VI) concentration in the wastewater exceeded the integrated wastewater discharge standard of China (GB 8978-1996) [39]. However, after adsorption, it was found that the removal efficiency of the total Cr and Cr(VI) by FeBC reached 93.36% and 96.77%, respectively. Both the concentration of total Cr and Cr(VI) in the wastewater were in compliance with the standard. After the adsorption treatment, the wastewater was drained into the city sewage pipe and continued to be treated. In addition, modified biochar also have the potential to remove chromium (Cr) from different actual wastewater. Yan Yang et al. [14] investigated the feasibility of FSBC to adsorb Cr in actual tanning wastewater. After adsorbing, the total Cr and Cr(VI) removal efficiency reached 98.50% and 99.60%, respectively, and the concentration of total Cr and Cr(VI) all were in standard.

**Table 4.** Cr removal capability of FeBC from actual wastewater.

| Condition | pH | Total Cr ($mg \cdot L^{-1}$) | Cr(VI) ($mg \cdot L^{-1}$) | Ni ($mg \cdot L^{-1}$) |
|---|---|---|---|---|
| Before adsorption | 6.2 | 19.89 ± 0.35 | 10.85 ± 0.11 | 0.48 ± 0.051 |
| After adsorption | 7.8 | 1.32 ± 0.07 | 0.35 ± 0.076 | 0.27 ± 0.021 |
| Standard limit | 6–9 | 1.5 | 0.5 | 1.0 |

Some studies indicate that alkali solution or $Na_2EDTA$ solution can desorb Cr from FeBC [14,40,41], which may help to realize the recycling and reuse of the adsorbent. The Cr (VI) removal rate decreases as the adsorption cycles increase. Finally, the inefficient adsorbent with toxic Cr is included in hazardous waste management and collected for incineration treatment. After incineration, ash containing chromium is collected for recycling.

## 4. Conclusions

In this study, FeBC was prepared by the impregnation method using rice straw biochar. Material characterization shows that iron oxides were loaded on the surface of FeBC, which had more active sites than that of BC. The surface functional groups of FeBC also changed, facilitating the removal of Cr(VI). Adsorption experiments showed that the removal efficiency of Cr(VI) by FeBC was significantly improved from 4.57% to 99.5%.

The adsorption efficiency was closely related to the mass modifier ratio, initial solution concentration and pH value. In addition, the presence of coexisting ions showed different degrees of inhibition. The isotherms and kinetics of Cr(VI) adsorption on FeBC were better described by the Langmuir isotherm and pseudo-second-order kinetic model, respectively. The study on adsorption mechanisms revealed that the Cr(VI) removal process by FeBC was accompanied by the electrostatic adsorption and the redox reaction of Cr. The reduction process was the main mechanism of the Cr(VI) removal by FeBC; Fe loaded on BC enhanced the Cr(VI) reduction process. This study will provide a theoretical basis for the Cr(VI) removal by FeBC; FeBC could be used as an efficient adsorbent for the Cr(VI) removal from aqueous solutions.

**Author Contributions:** Methodology, J.B.; formal analysis, Z.Z. and G.R.; data curation, K.L.; writing—original draft preparation, R.P.; writing—review and editing, A.D. All authors have read and agreed to the published version of the manuscript.

**Funding:** This research was funded by Jiangsu Provincial Department of Education, grant number No. 202011460063Y.

**Data Availability Statement:** The data presented in this study are available upon request from the corresponding author.

**Conflicts of Interest:** The authors declare no conflict of interest.

## References


1. Bagchi, D.; Stohs, S.J.; Downs, B.W.; Bagchi, M.; Preuss, H.G. Cytotoxicity and oxidative mechanisms of different forms of chromium. *Toxicology* **2002**, *180*, 5–22. [CrossRef]
2. Oliveira, H.; Spano, M.; Guevara, M.A.; Santos, T.M.; Santos, C.; Pereira, M.D. Evaluation of in vivo reproductive toxicity of potassium chromate in male mice. *Exp. Toxicol. Pathol.* **2010**, *62*, 391–404. [CrossRef]
3. Nur-E-Alam, M.; Mia, M.A.S.; Ahmad, F.; Rahman, M.M. Adsorption of chromium (Cr) from tannery wastewater using low-cost spent tea leaves adsorbent. *Appl. Water Sci.* **2018**, *8*, 129. [CrossRef]
4. Jiang, S.; Yan, X.; Peacock, C.L.; Zhang, S.; Li, W.; Zhang, J.; Feng, X.; Liu, F.; Yin, H. Adsorption of Cr(VI) on Al-substituted hematites and its reduction and retention in the presence of $Fe^{2+}$ under conditions similar to subsurface soil environments. *J. Hazard. Mater.* **2020**, *390*, 122014. [CrossRef]
5. Cely, P.; Gasco, G.; Paz-Ferreiro, J.; Mendez, A. Agronomic properties of biochars from different manure wastes. *J. Anal. Appl. Pyrol.* **2015**, *111*, 173–182. [CrossRef]
6. Iamsaard, K.; Weng, C.-H.; Yen, L.-T.; Tzeng, J.-H.; Poonpakdee, C.; Lin, Y.-T. Adsorption of metal on pineapple leaf biochar: Key affecting factors, mechanism identification, and regeneration evaluation. *Bioresour. Technol.* **2021**, *344*, 126131. [CrossRef] [PubMed]
7. Xia, S.; Song, Z.; Jeyakumar, P.; Bolan, N.; Wang, H. Characteristics and applications of biochar for remediating Cr(VI)-contaminated soils and wastewater. *Environ. Geochem. Health* **2020**, *42*, 1543–1567. [CrossRef] [PubMed]
8. Li, R.H.; Wang, J.J.; Gaston, L.A.; Zhou, B.Y.; Li, M.L.; Xiao, R.; Wang, Q.; Zhang, Z.Q.; Huang, H.; Liang, W.; et al. An overview of carbothermal synthesis of metal-biochar composites for the removal of oxyanion contaminants from aqueous solution. *Carbon* **2018**, *129*, 674–687. [CrossRef]
9. Yu, Y.; An, Q.; Jin, L.; Luo, N.; Li, Z.; Jiang, J. Unraveling sorption of Cr (VI) from aqueous solution by $FeCl_3$ and $ZnCl_2$-modified corn stalks biochar: Implicit mechanism and application. *Bioresour. Technol.* **2020**, *297*, 122466. [CrossRef]
10. Lyu, H.H.; Tang, J.C.; Huang, Y.; Gai, L.S.; Zeng, E.Y.; Liber, K.; Gong, Y.Y. Removal of hexavalent chromium from aqueous solutions by a novel biochar supported nanoscale iron sulfide composite. *Chem. Eng. J.* **2017**, *322*, 516–524. [CrossRef]
11. Zhu, Y.; Li, H.; Zhang, G.; Meng, F.; Li, L.; Wu, S. Removal of hexavalent chromium from aqueous solution by different surface-modified biochars: Acid washing, nanoscale zero-valent iron and ferric iron loading. *Bioresour. Technol.* **2018**, *261*, 142–150. [CrossRef]
12. Pan, J.-j.; Jiang, J.; Xu, R.-K. Removal of Cr(VI) from aqueous solutions by $Na_2SO_3$/$FeSO_4$ combined with peanut straw biochar. *Chemosphere* **2014**, *101*, 71–76. [CrossRef]
13. Dong, X.; Ma, L.Q.; Li, Y. Characteristics and mechanisms of hexavalent chromium removal by biochar from sugar beet tailing. *J. Hazard. Mater.* **2011**, *190*, 909–915. [CrossRef] [PubMed]
14. Yang, Y.; Zhang, Y.; Wang, G.; Yang, Z.; Xian, J.; Yang, Y.; Li, T.; Pu, Y.; Jia, Y.; Li, Y. Adsorption and reduction of Cr (VI) by a novel nanoscale FeS/chitosan/biochar composite from aqueous solution. *J. Environ. Chem. Eng.* **2021**, *9*, 105407. [CrossRef]
15. Choudhary, B.; Paul, D. Isotherms, kinetics and thermodynamics of hexavalent chromium removal using biochar. *J. Environ. Chem. Eng.* **2018**, *6*, 2335–2343. [CrossRef]
16. Reguyal, F.; Sarmah, A.K.; Gao, W. Synthesis of magnetic biochar from pine sawdust via oxidative hydrolysis of $FeCl_2$ for the removal sulfamethoxazole from aqueous solution. *J. Hazard. Mater.* **2017**, *321*, 868–878. [CrossRef]
17. Yi, Y.; Wang, X.; Ma, J.; Ning, P. An efficient Egeria najas-derived biochar supported nZVI composite for Cr (VI) removal: Characterization and mechanism investigation based on visual MINTEQ model. *Environ. Res.* **2020**, *189*, 109912. [CrossRef]
18. Cho, D.-W.; Yoon, K.; Kwon, E.E.; Biswas, J.K.; Song, H. Fabrication of magnetic biochar as a treatment medium for As (V) via pyrolysis of FeCl3-pretreated spent coffee ground. *Environ. Pollut.* **2017**, *229*, 942–949. [CrossRef] [PubMed]
19. Pan, J.J.; Jiang, J.; Xu, R.K. Adsorption of Cr(III) from acidic solutions by crop straw derived biochars. *J. Environ. Sci.* **2013**, *25*, 1957–1965. [CrossRef]
20. Guo, Y.; Tang, W.; Wu, J.G.; Huang, Z.Q.; Dai, J.Y. Mechanism of Cu(II) adsorption inhibition on biochar by its aging process. *J. Environ. Sci.* **2014**, *26*, 2123–2130. [CrossRef]
21. Yuan, Y.; Bolan, N.; Prevoteau, A.; Vithanage, M.; Biswas, J.K.; Ok, Y.S.; Wang, H.L. Applications of biochar in redox-mediated reactions. *Bioresour. Technol.* **2017**, *246*, 271–281. [CrossRef]
22. Nakarmi, A.; Bourdo, S.E.; Ruhl, L.; Kanel, S.; Nadagouda, M.; Alla, P.K.; Pavel, I.; Viswanathan, T. Benign zinc oxide betaine-modified biochar nanocomposites for phosphate removal from aqueous solutions. *J. Environ. Manag.* **2020**, *272*, 111048. [CrossRef]
23. Huang, Z.; Dai, X.; Huang, Z.; Wang, T.; Cui, L.; Ye, J.; Wu, P. Simultaneous and efficient photocatalytic reduction of Cr(VI) and oxidation of trace sulfamethoxazole under LED light by rGO@$Cu_2O$/$BiVO_4$ p-n heterojunction composite. *Chemosphere* **2019**, *221*, 824–833. [CrossRef]
24. Dong, H.R.; Deng, J.M.; Xie, Y.K.; Zhang, C.; Jiang, Z.; Cheng, Y.J.; Hou, K.J.; Zeng, G.M. Stabilization of nanoscale zero-valent iron (nZVI) with modified biochar for Cr(VI) removal from aqueous solution. *J. Hazard. Mater.* **2017**, *332*, 79–86. [CrossRef]
25. Choudhary, B.; Paul, D.; Singh, A.; Gupta, T. Removal of hexavalent chromium upon interaction with biochar under acidic conditions: Mechanistic insights and application. *Environ. Sci. Pollut. Res.* **2017**, *24*, 16786–16797. [CrossRef]
26. Sass, B.M.; Rai, D. Solubility of amorphous chromium(III)-iron(III) hydroxide solid-solutions. *Inorg. Chem.* **1987**, *26*, 2228–2232. [CrossRef]

27. Deng, J.; Li, X.; Wei, X.; Liu, Y.; Liang, J.; Shao, Y.; Huang, W.; Cheng, X. Different adsorption behaviors and mechanisms of a novel amino-functionalized hydrothermal biochar for hexavalent chromium and pentavalent antimony. *Bioresour. Technol.* **2020**, *310*, 123438. [CrossRef] [PubMed]
28. Zhang, J.S.; Chen, S.J.; Zhang, H.W.; Wang, X.K. Removal behaviors and mechanisms of hexavalent chromium from aqueous solution by cephalosporin residue and derived chars. *Bioresour. Technol.* **2017**, *238*, 484–491. [CrossRef] [PubMed]
29. Lyonga, F.N.; Hong, S.H.; Cho, E.J.; Kang, J.K.; Lee, C.G.; Park, S.J. As(III) adsorption onto Fe-impregnated food waste biochar: Experimental investigation, modeling, and optimization using response surface methodology. *Environ. Geochem. Health* **2021**, *43*, 3303–3321. [CrossRef]
30. Gan, C.; Liu, Y.G.; Tan, X.F.; Wang, S.F.; Zeng, G.M.; Zheng, B.H.; Li, T.T.; Jiang, Z.J.; Liu, W. Effect of porous zinc-biochar nanocomposites on Cr(VI) adsorption from aqueous solution. *RSC Adv.* **2015**, *5*, 35107–35115. [CrossRef]
31. Nethaji, S.; Sivasamy, A.; Mandal, A.B. Preparation and characterization of corn cob activated carbon coated with nano-sized magnetite particles for the removal of Cr(VI). *Bioresour. Technol.* **2013**, *134*, 94–100. [CrossRef]
32. Li, T.T.; Liu, Y.G.; Peng, Q.Q.; Hu, X.J.; Liao, T.; Wang, H.; Lu, M. Removal of lead(II) from aqueous solution with ethylenediamine-modified yeast biomass coated with magnetic chitosan microparticles: Kinetic and equilibrium modeling. *Chem. Eng. J.* **2013**, *214*, 189–197. [CrossRef]
33. Zhang, T.; Xu, H.Y.; Li, H.H.; He, X.Y.; Shi, Y.J.; Kruse, A. Microwave digestion-assisted HFO/biochar adsorption to recover phosphorus from swine manure. *Sci. Total Environ.* **2018**, *621*, 1512–1526. [CrossRef] [PubMed]
34. Venkateswarlu, S.; Lee, D.; Yoon, M. Bioinspired 2D-Carbon Flakes and $Fe_3O_4$ Nanoparticles Composite for Arsenite Removal. *Acs Appl. Mater. Inter.* **2016**, *8*, 23876–23885. [CrossRef] [PubMed]
35. Liu, N.; Zhang, Y.T.; Xu, C.; Liu, P.; Lv, J.; Liu, Y.Y.; Wang, Q.Y. Removal mechanisms of aqueous Cr(VI) using apple wood biochar: A spectroscopic study. *J. Hazard. Mater.* **2020**, *384*, 121371. [CrossRef]
36. Lyu, H.H.; Zhao, H.; Tang, J.C.; Gong, Y.Y.; Huang, Y.; Wu, Q.H.; Gao, B. Immobilization of hexavalent chromium in contaminated soils using biochar supported nanoscale iron sulfide composite. *Chemosphere* **2018**, *194*, 360–369. [CrossRef] [PubMed]
37. Wang, X.D.; Xu, J.; Liu, J.; Liu, J.; Xia, F.; Wang, C.C.; Dahlgren, R.A.; Liu, W. Mechanism of Cr(VI) removal by magnetic greigite/biochar composites. *Sci. Total Environ.* **2020**, *700*, 134414. [CrossRef]
38. Hu, J.; Chen, G.; Lo, I.M. Removal and recovery of Cr(VI) from wastewater by maghemite nanoparticles. *Water Res.* **2005**, *39*, 4528–4536. [CrossRef]
39. CHINA. Integrated Wastewater Discharge Standard GB/T 8978. 1996. Available online: https://www.mee.gov.cn/ywgz/fgbz/bz/bzwb/shjbh/swrwpfbz/199801/t19980101_66568.htm (accessed on 1 October 2021).
40. Kołodyńska, D.; Krukowska, J.; Thomas, P. Comparison of sorption and desorption studies of heavy metal ions from biochar and commercial active carbon. *Chem. Eng. J.* **2017**, *307*, 353–363. [CrossRef]
41. Ding, Z.; Hu, X.; Wan, Y.; Wang, S.; Gao, B. Removal of lead, copper, cadmium, zinc, and nickel from aqueous solutions by alkali-modified biochar: Batch and column tests. *J. Ind. Eng. Chem.* **2016**, *33*, 239–245. [CrossRef]